

Supporting Information

Kinetic Study of Catalytic Formic Acid Dehydrogenation by in Situ UV-Vis Spectroscopy

Seo Ono,^{a,b} Risheng Li,^{a,b} Chieko Suzuki,^c Akira Yamamoto,^d Hisao Yoshida,^d Hajime Kawanami,^{a,b}
Ryoichi Kanega^{*c}

^aResearch Center for Catalytic Chemistry, National Institute of Advanced Industrial Science and Technology, Tsukuba Central 5, 1-1-1 Higashi, Tsukuba, Ibaraki, 305-8565, Japan

^bGraduate School of Pure and Applied Science Interdisciplinary, University of Tsukuba, Tsukuba, Ibaraki, 305-8577, Japan

^cResearch Institute for Energy Conservation, National Institute of Advanced Industrial Science and Technology, Tsukuba Central 5, 1-1-1 Higashi, Tsukuba, Ibaraki, 305-8565, Japan

^dDepartment of Interdisciplinary Environment, Graduate School of Human and Environmental Studies, Kyoto University, Yoshida Nihonmatsu-cho, Sakyo-ku, Kyoto 606-8501, Japan

*Correspondence to: r-kanega@aist.go.jp

Table of Contents

Figures S1 to S34

S2-S18

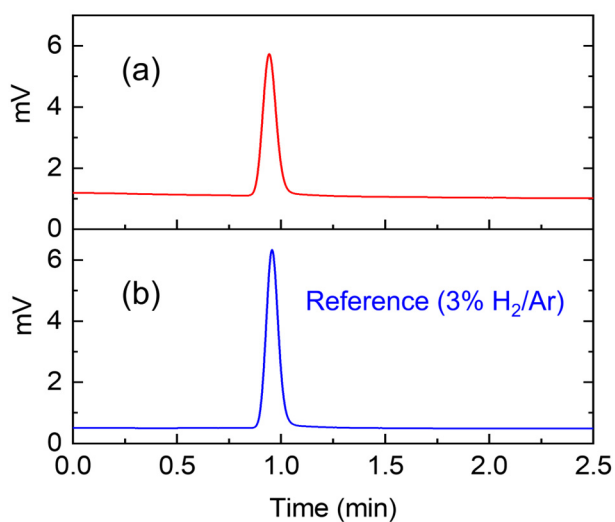


Figure S1. GC-TCD chromatographs of (a) gas product after addition of H_2SO_4 and (b) reference (3% H_2/Ar , 0.5 mL).

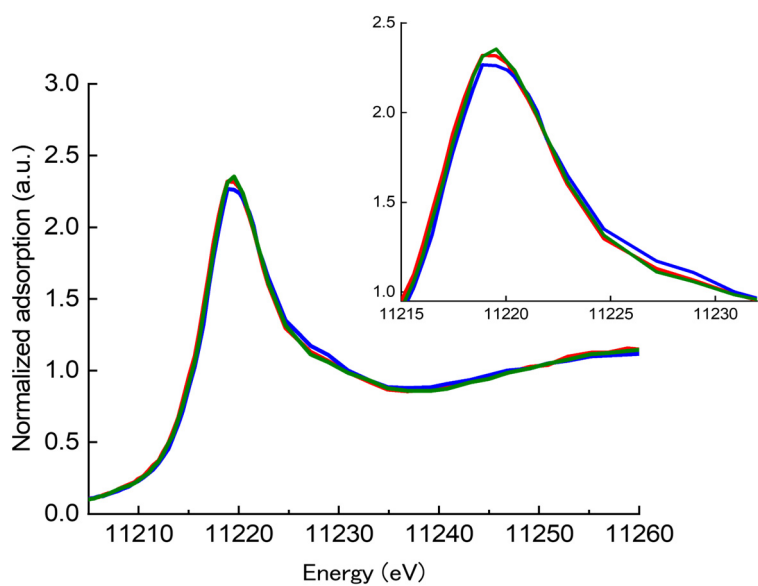


Figure S2. Normalized XANES spectra of **Ir3** solution (red line), **Ir3**/ HCO_2K solution (blue line), **Ir3**/ $\text{HCO}_2\text{K}/\text{H}_2\text{SO}_4$ solution (green line).

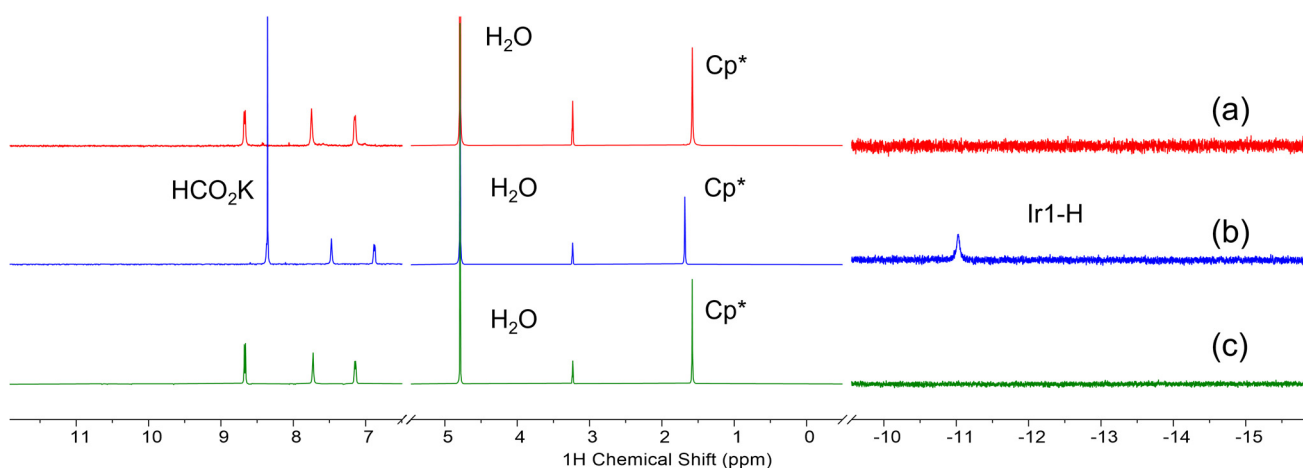


Figure S3. ^1H NMR spectra of **Ir1** (expanded to 50 times for below -10 ppm and 10 times for above 7 ppm). (a) **Ir1** in $\text{D}_2\text{O}/\text{CD}_3\text{OD}$ (7/3), (b) **Ir1** with 5 equiv. of HCO_2K in $\text{D}_2\text{O}/\text{CD}_3\text{OD}$ (7/3), (c) Addition of 5 equiv. of D_2SO_4 to (b).

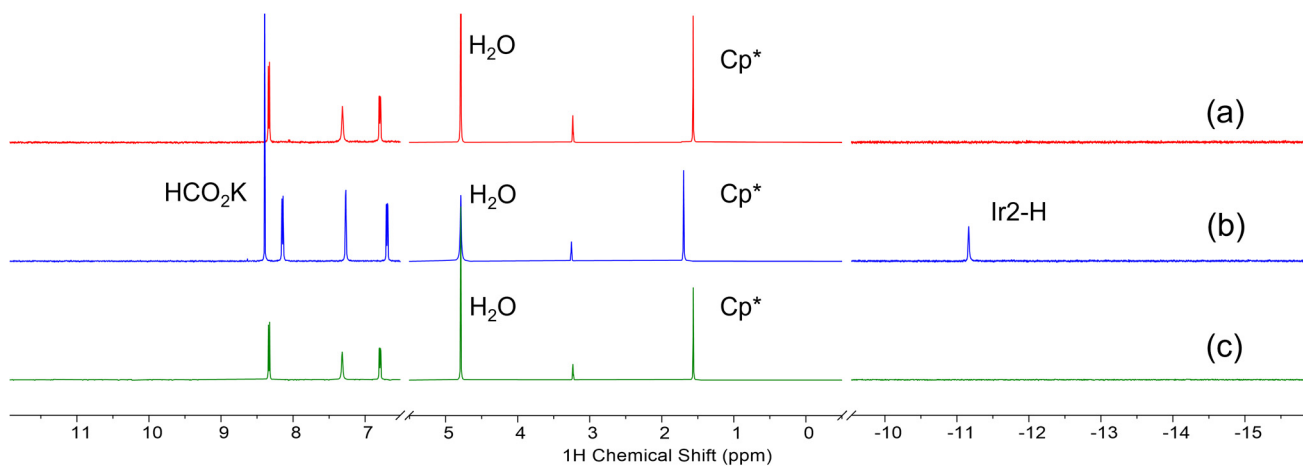


Figure S4. ^1H NMR spectra of **Ir2** (expanded to 50 times for below -10 ppm and 10 times for above 7 ppm). (a) **Ir2** in $\text{D}_2\text{O}/\text{CD}_3\text{OD}$ (7/3), (b) **Ir2** with 5 equiv. of HCO_2K in $\text{D}_2\text{O}/\text{CD}_3\text{OD}$ (7/3), (c) Addition of 5 equiv. of D_2SO_4 to (b).

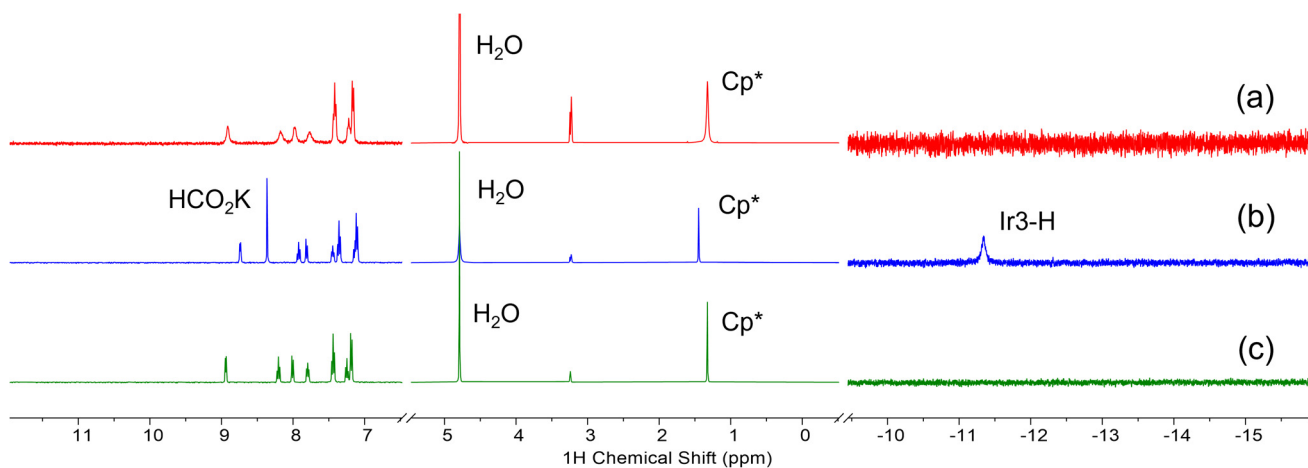


Figure S5. ^1H NMR spectra of Ir3 (expanded to 50 times for below -10 ppm and 10 times for above 7 ppm). (a) Ir3 in $\text{D}_2\text{O}/\text{CD}_3\text{OD}$ (7/3), (b) Ir3 with 5 equiv. of HCO_2K in $\text{D}_2\text{O}/\text{CD}_3\text{OD}$ (7/3), (c) Addition of 5 equiv. of D_2SO_4 to (b).

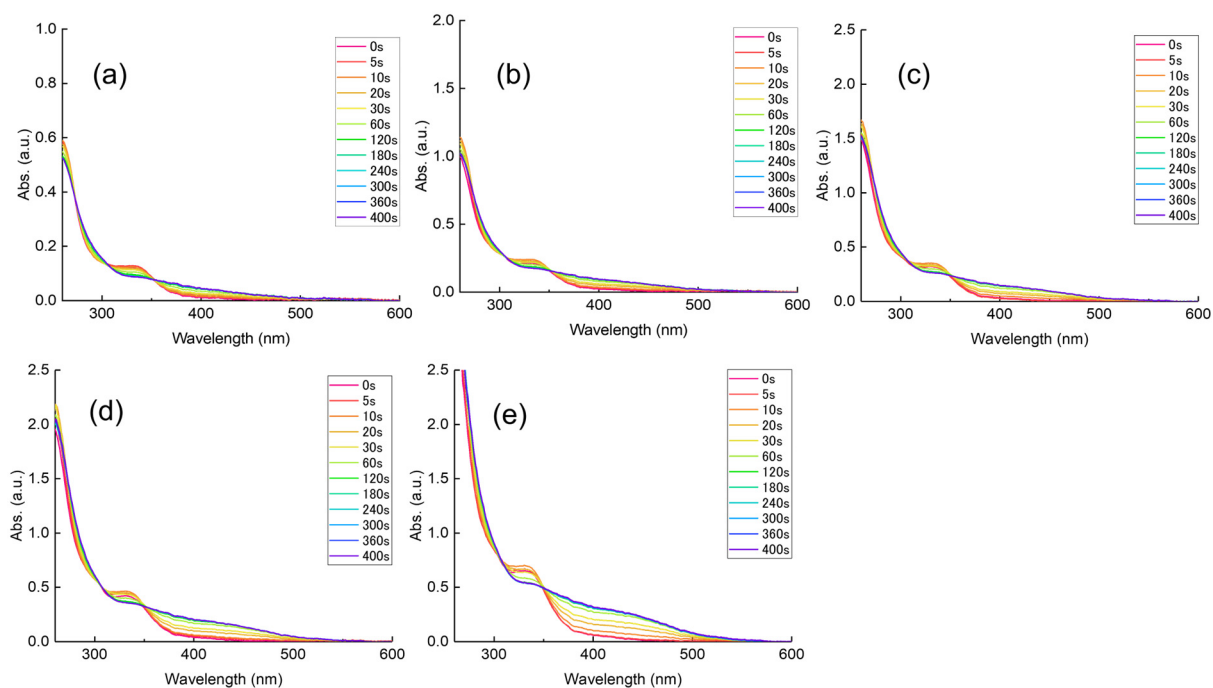


Figure S6. UV-vis spectra of Ir1 with the addition of HCO_2K .

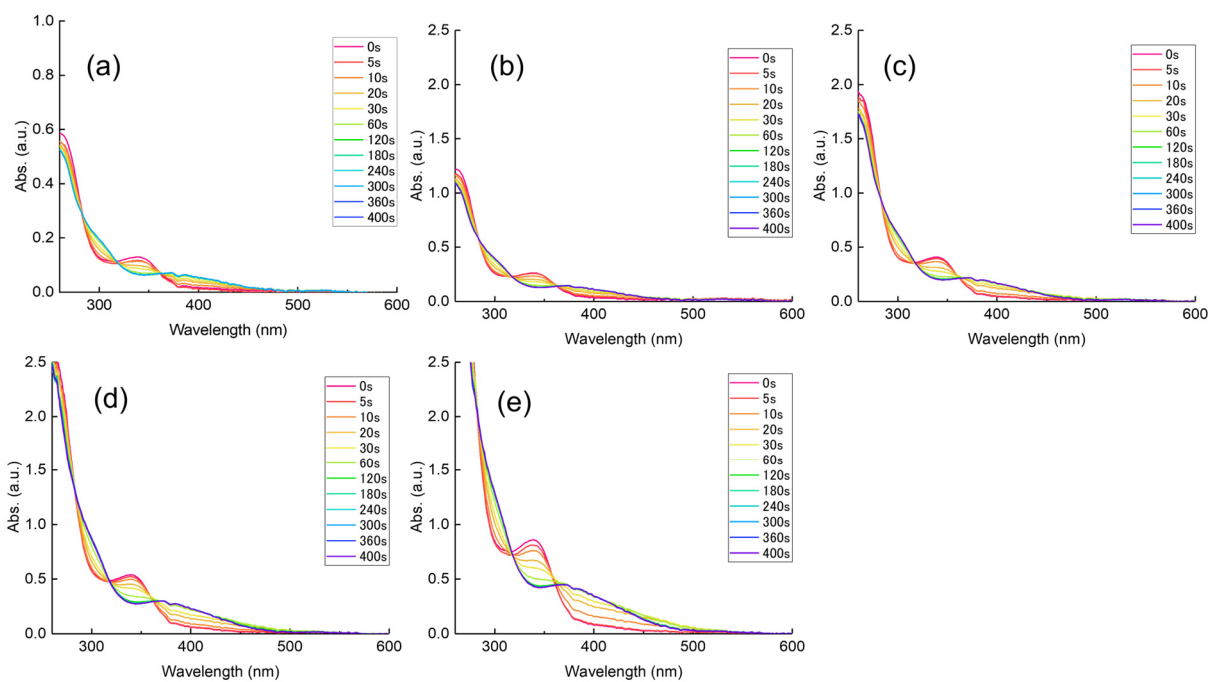


Figure S7. UV-vis spectra of Ir2 with the addition of HCO₂K.

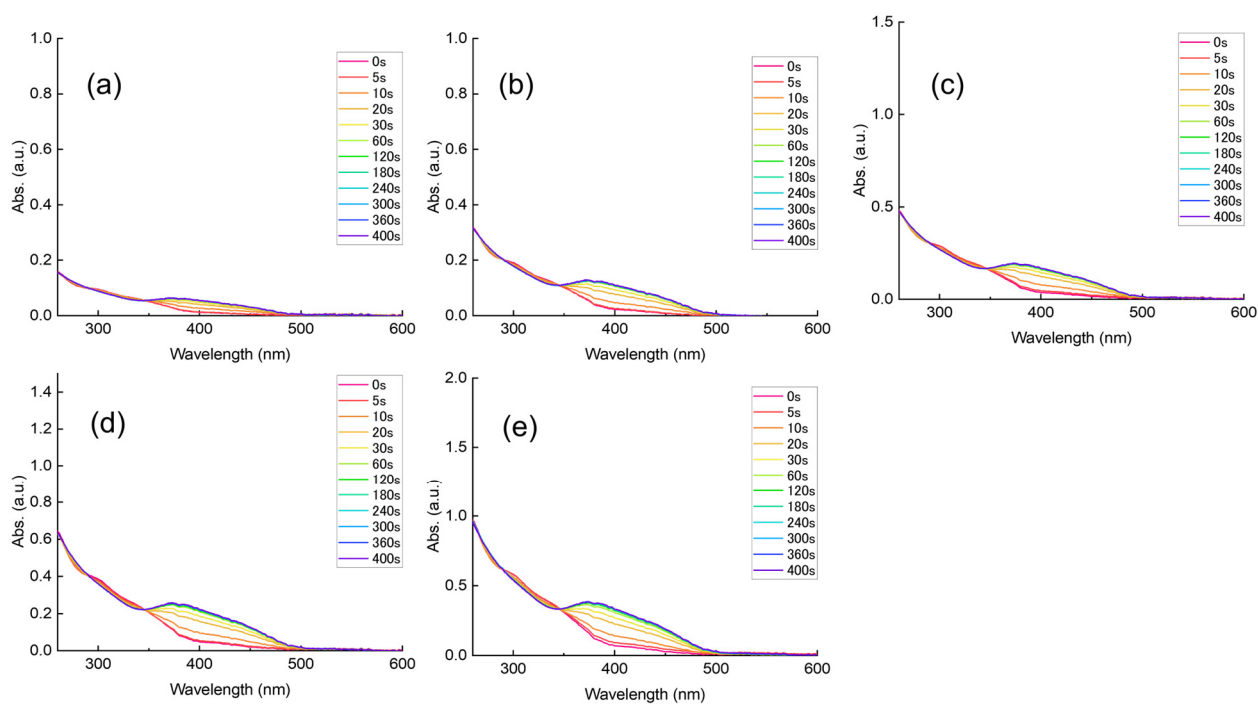


Figure S8. UV-vis spectra of Ir3 with the addition of HCO₂K.

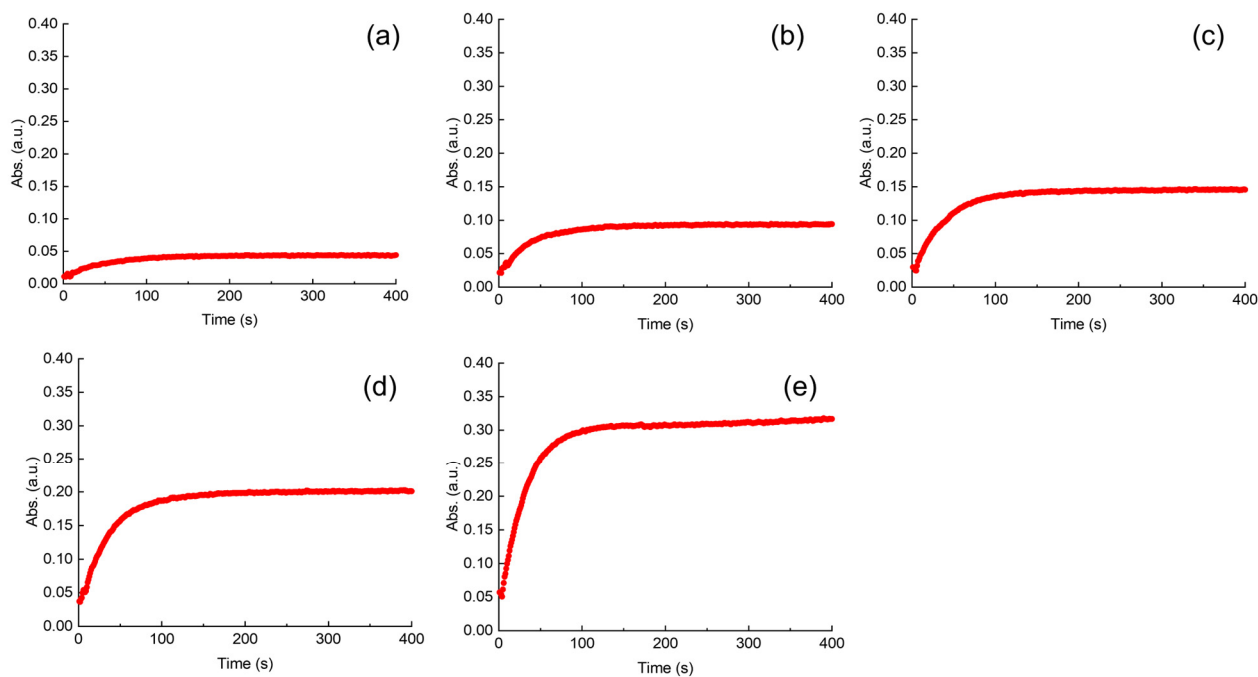


Figure S9. Time course of absorption at 400 nm with various concentration of Ir1.

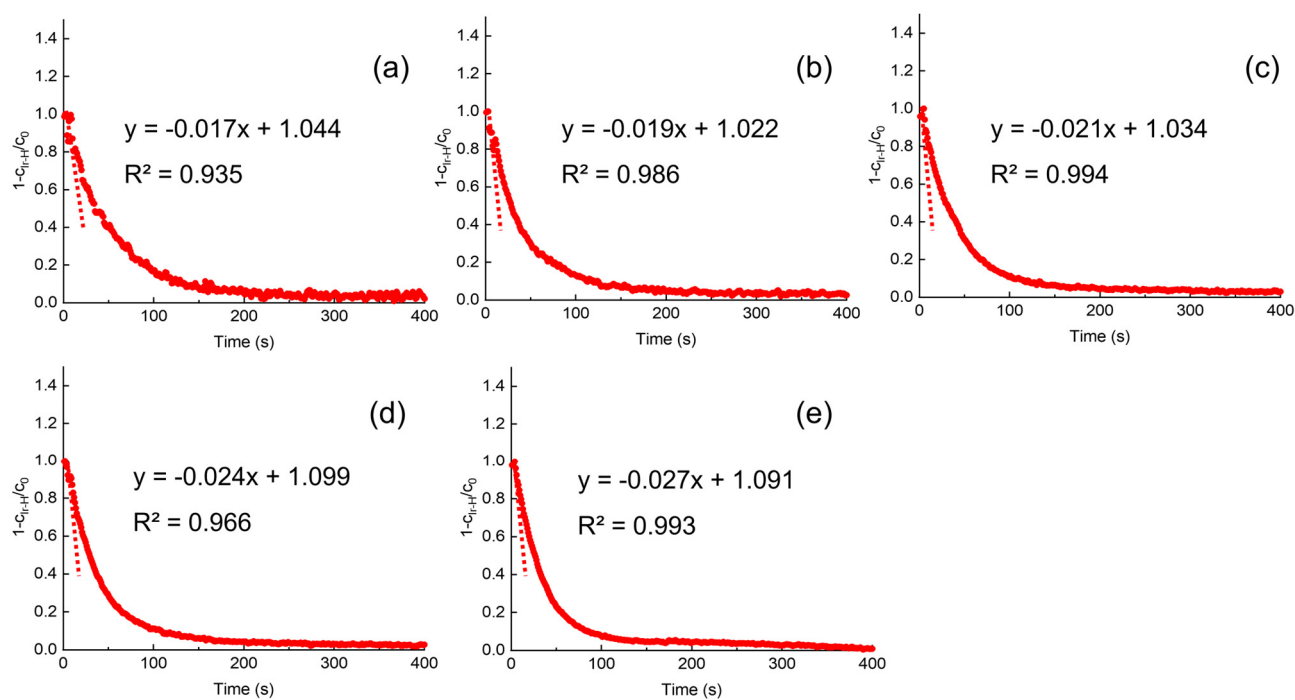


Figure S10. The initial hydride formation rates with various concentration of Ir1.

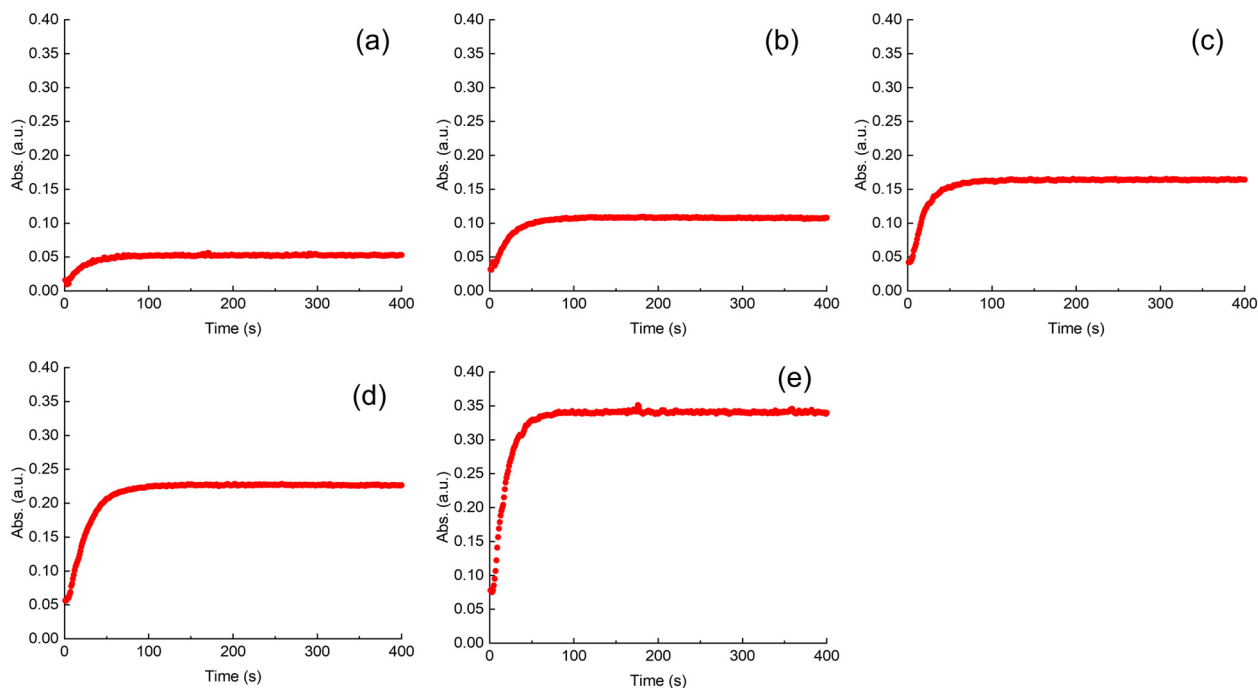


Figure S11. Time course of absorption at 400 nm with various concentration of Ir2.

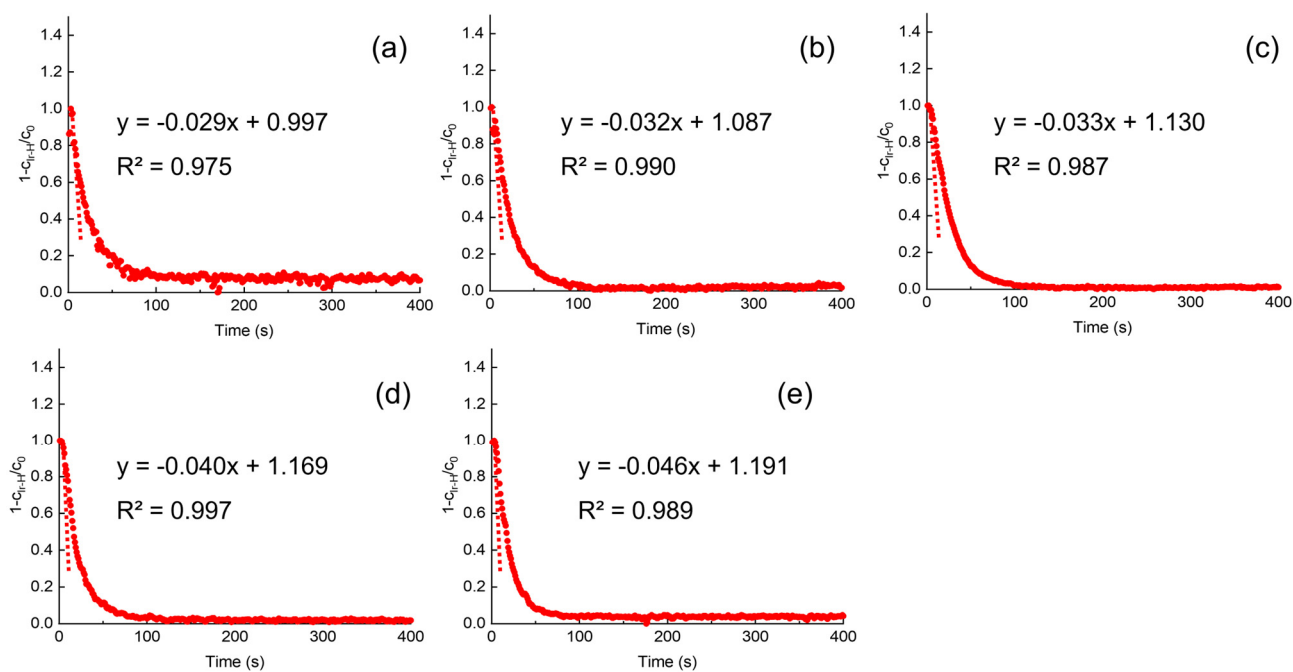


Figure S12. The initial hydride formation rates with various concentration of Ir2.

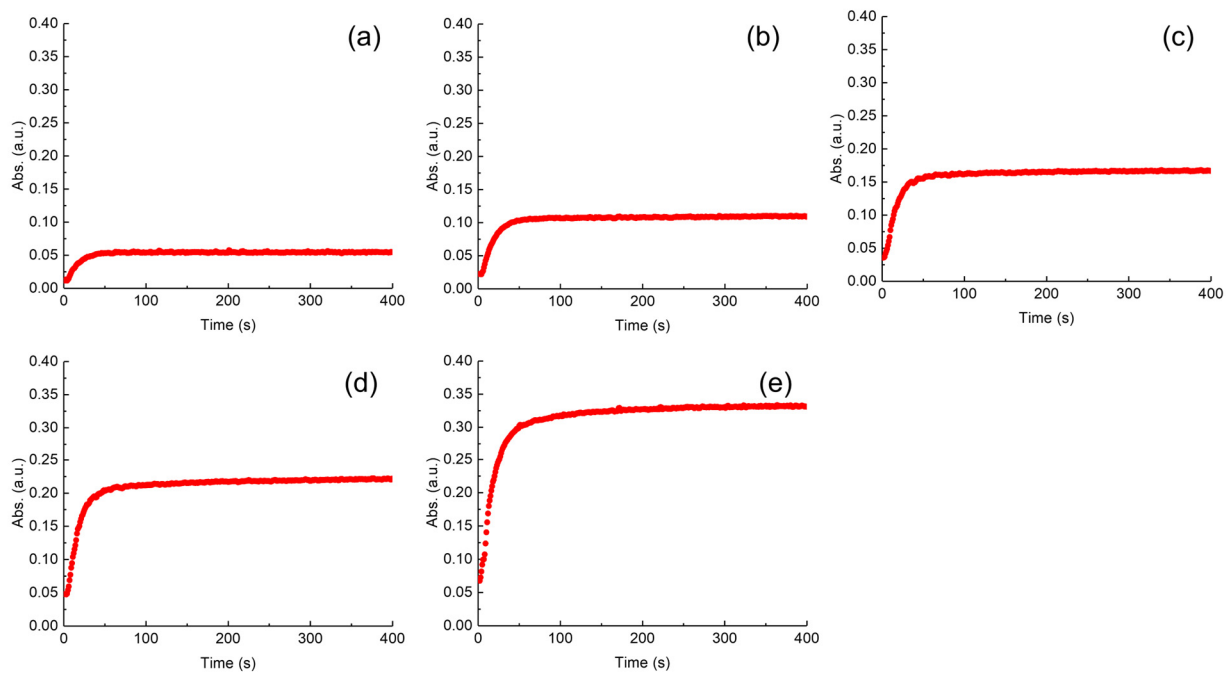


Figure S13. Time course of absorption at 400 nm with various concentration of Ir3.

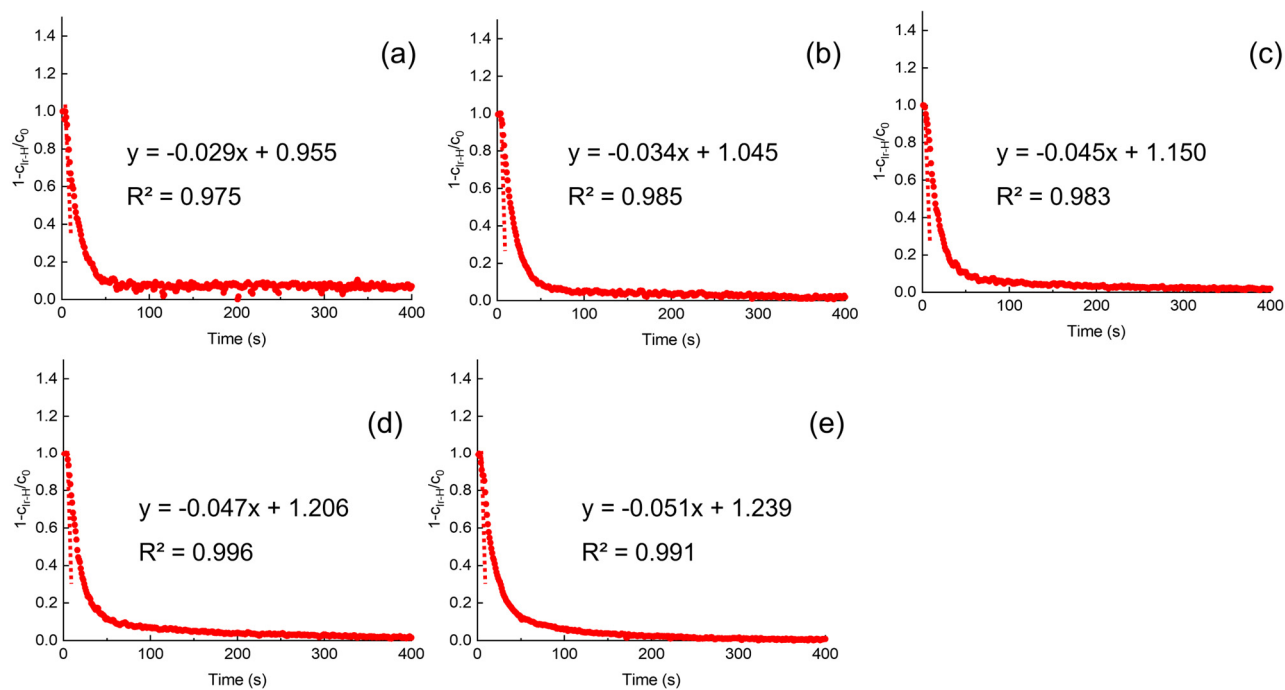


Figure S14. The initial hydride formation rates with various concentration of Ir3.

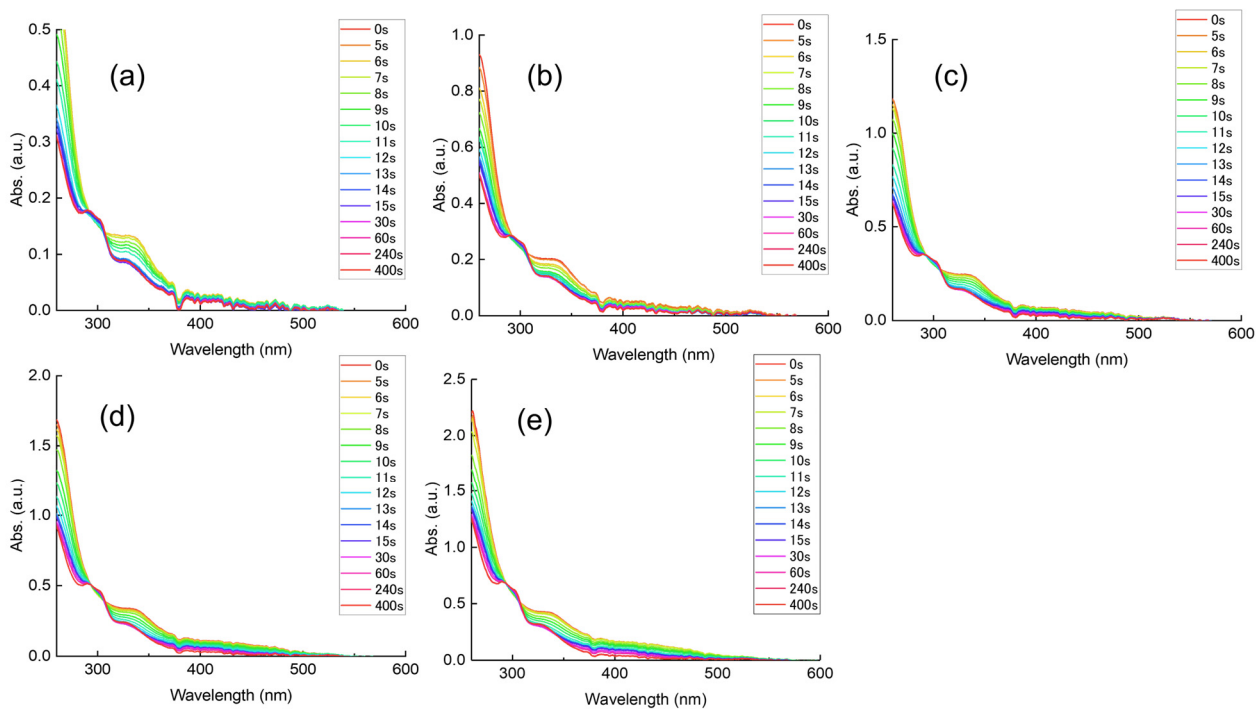


Figure S15. UV-vis spectra of Ir1 with the addition of HCO₂K and H₂SO₄.

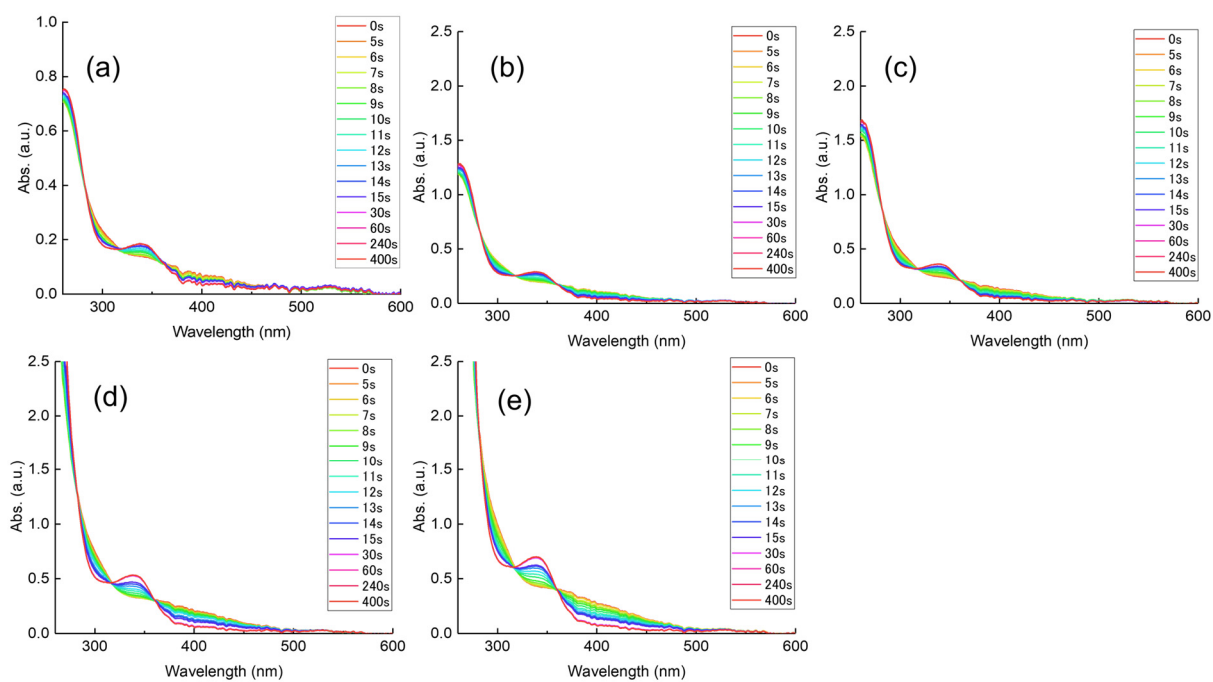


Figure S16. UV-vis spectra of Ir2 with the addition of HCO₂K and H₂SO₄.

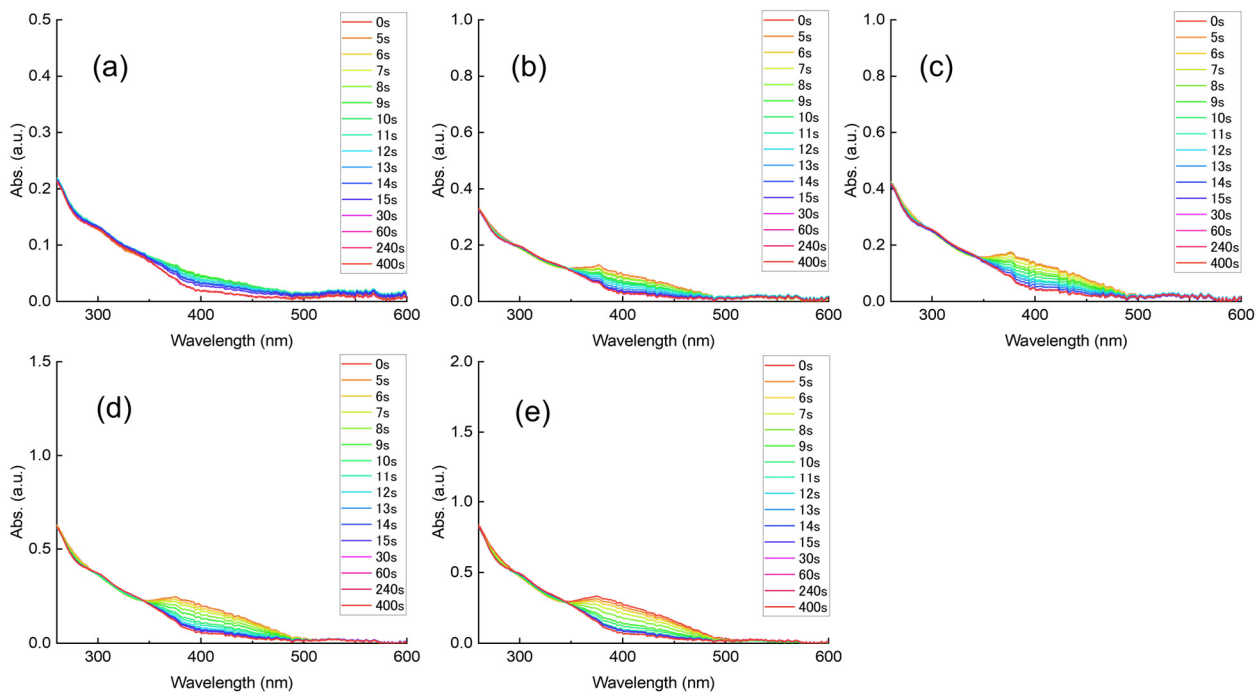


Figure S17. UV-vis spectra of Ir3 with the addition of HCO₂K and H₂SO₄.

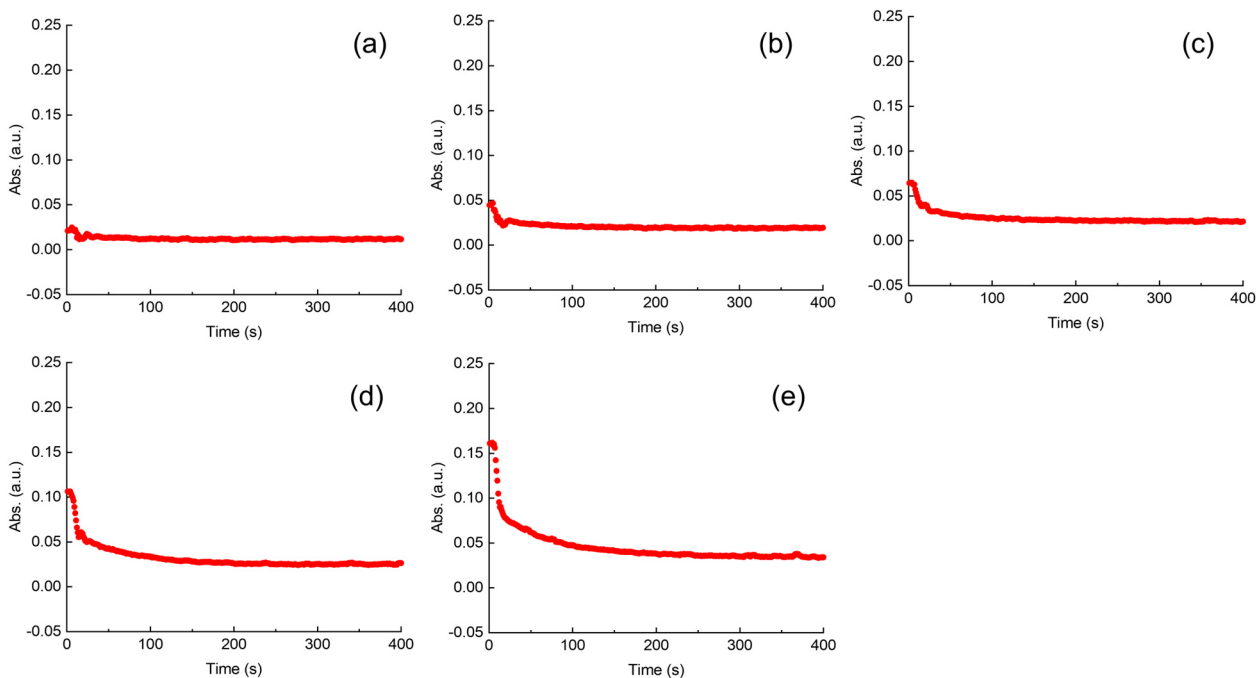


Figure S18. Time course of absorption at 400 nm with various concentration of Ir1.

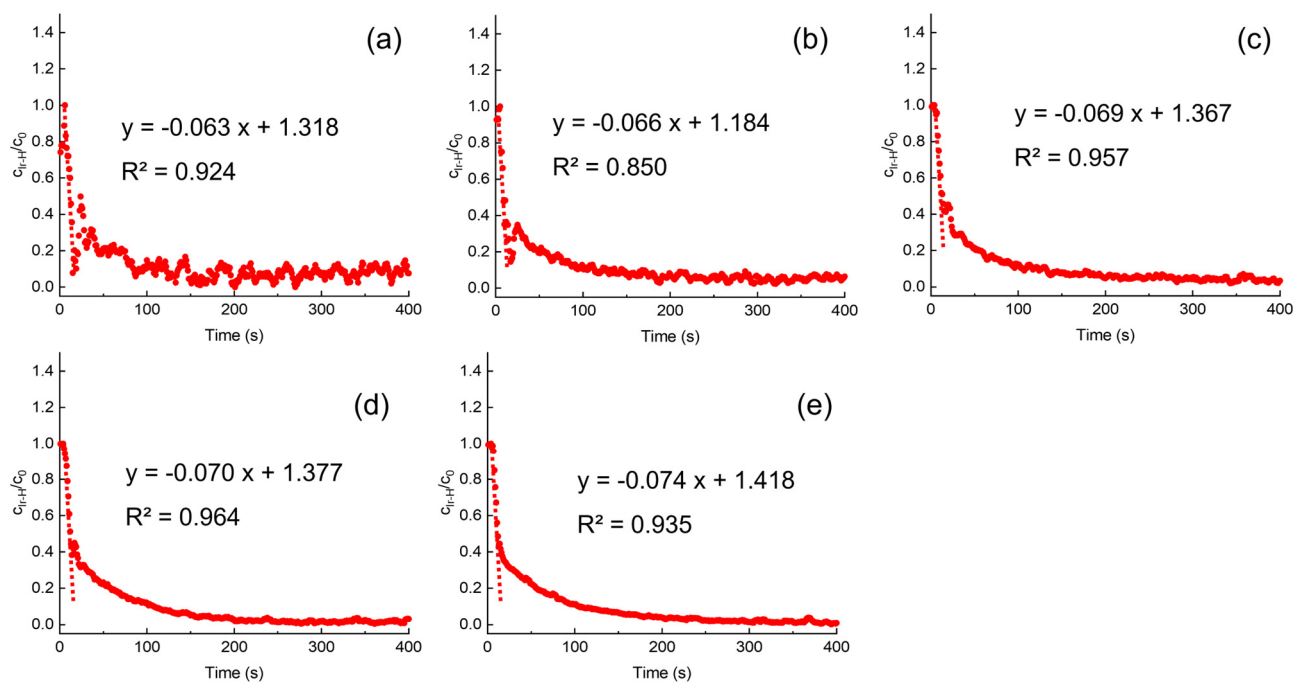


Figure S19. The initial H_2 evolution rates with various concentration of Ir1.

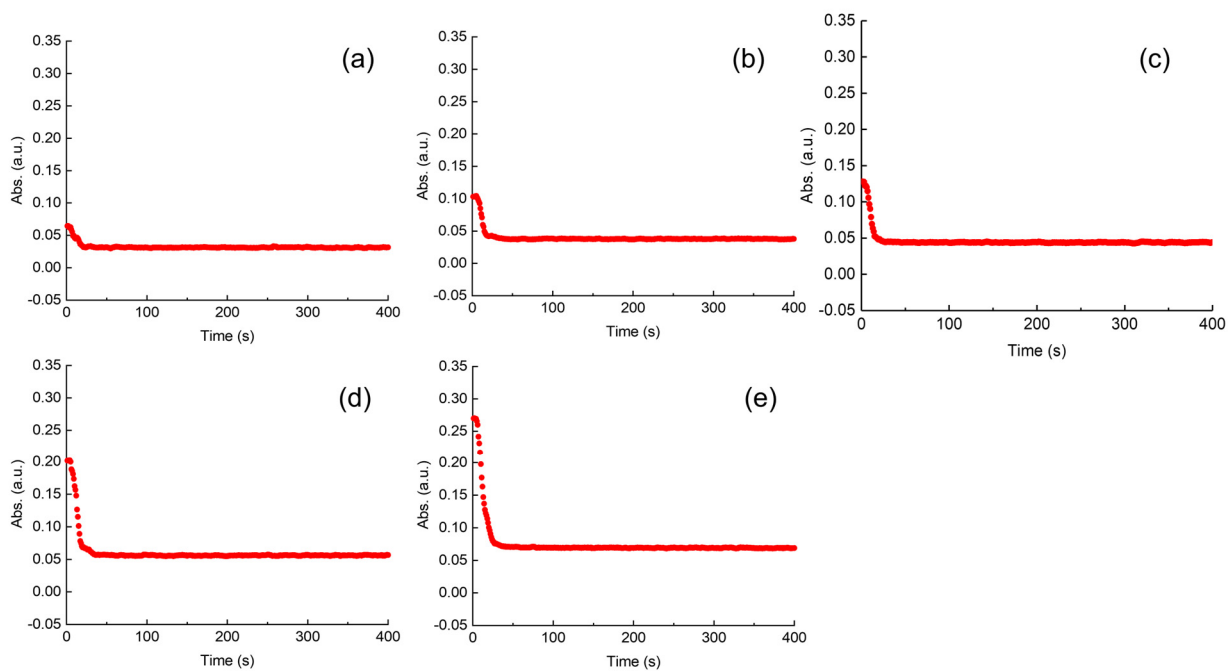


Figure S20. Time course of absorption at 400 nm with various concentration of Ir2.

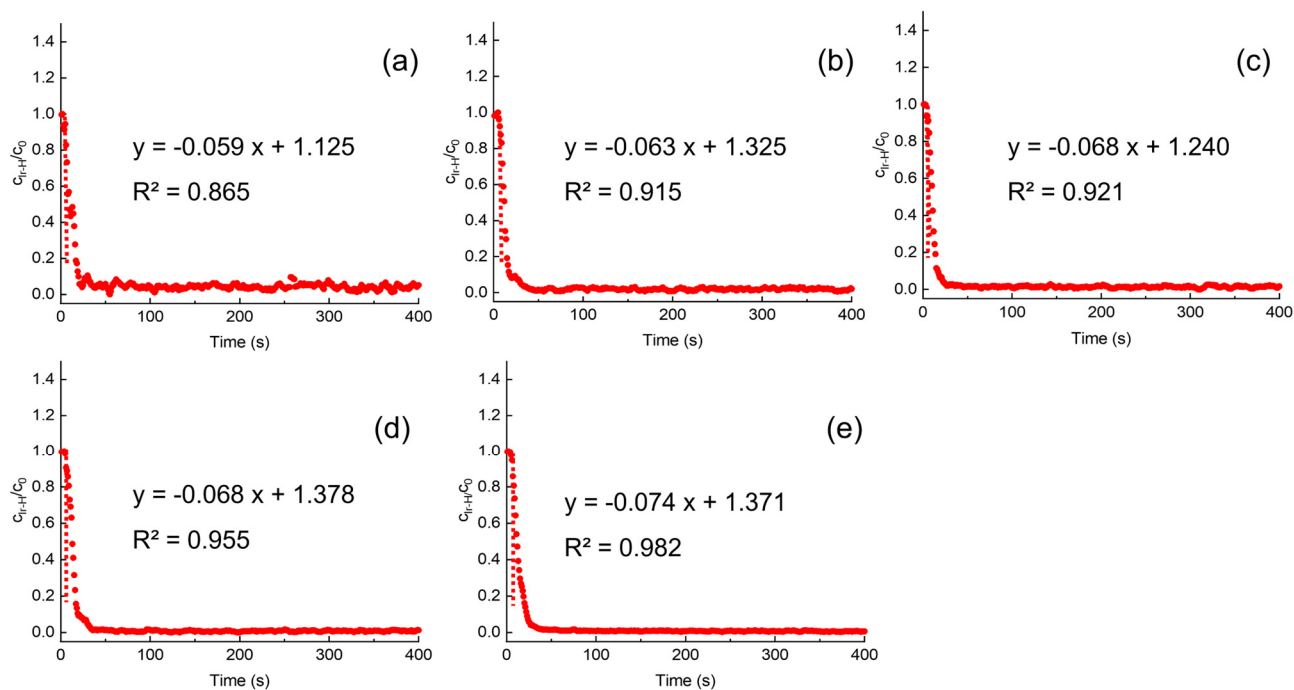


Figure S21. The initial H_2 evolution rates with various concentration of Ir2.

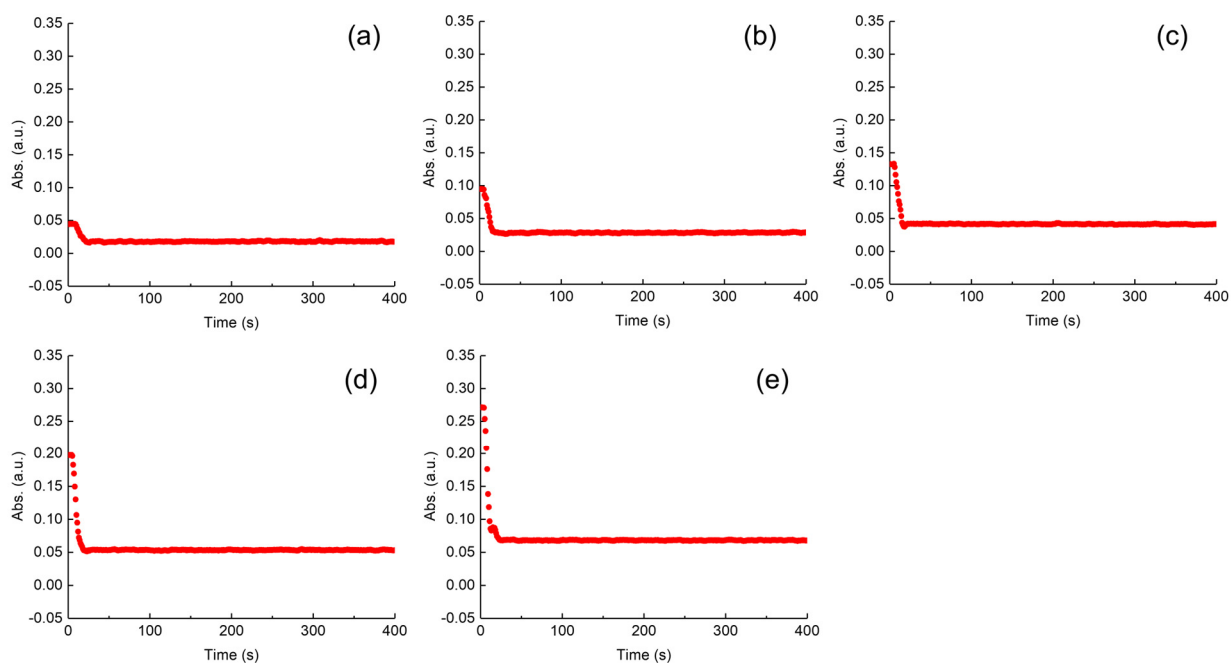


Figure S22. Time course of absorption at 400 nm with various concentration of Ir3.

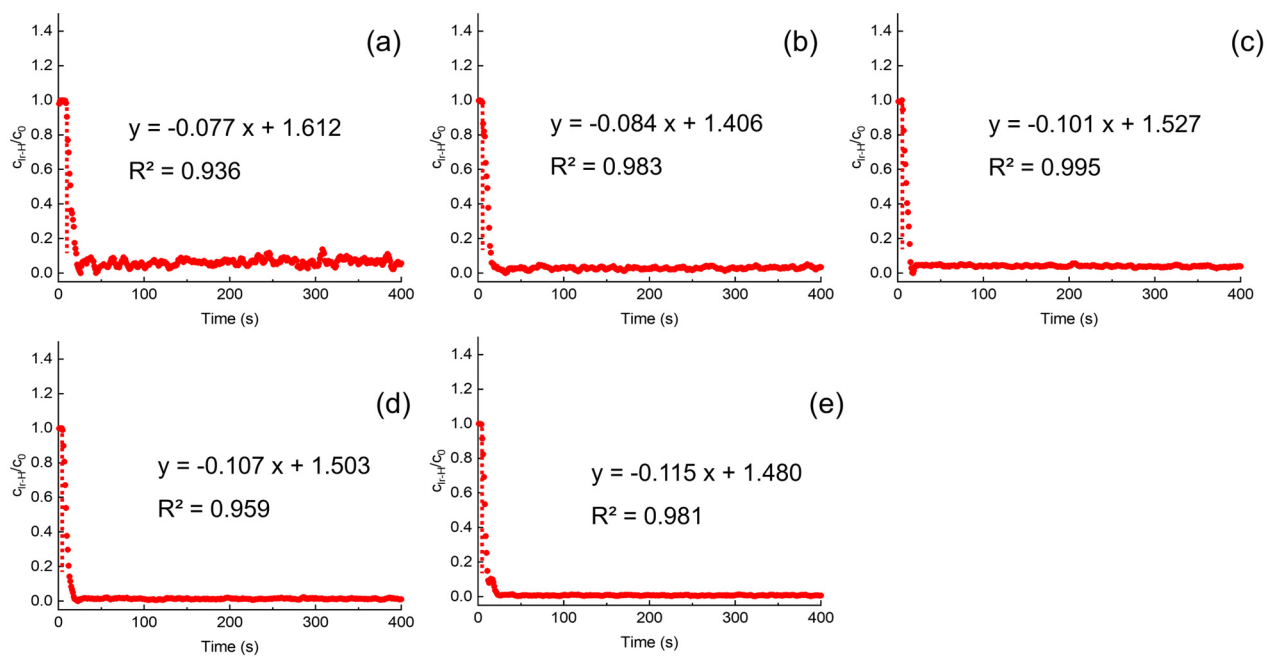


Figure S23. The initial H_2 evolution rates with various concentration of Ir3.

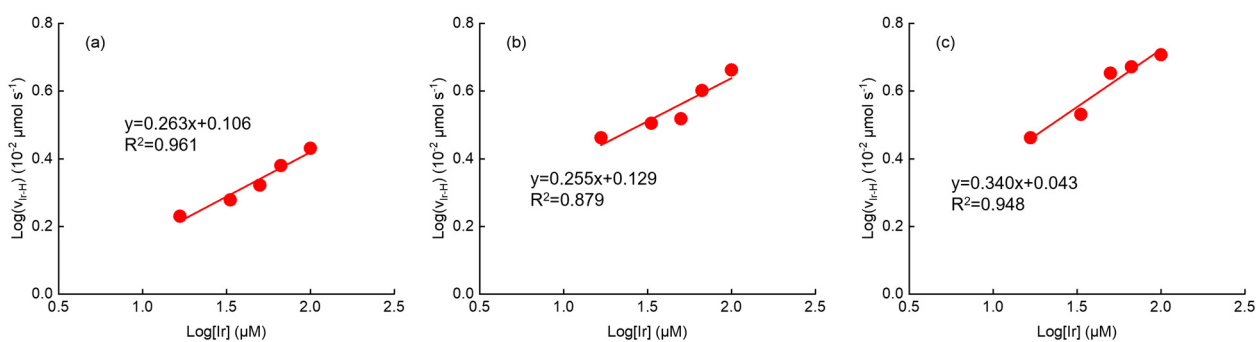


Figure S24. Reaction order of (a) Ir1, (b) Ir2, (c) Ir3.

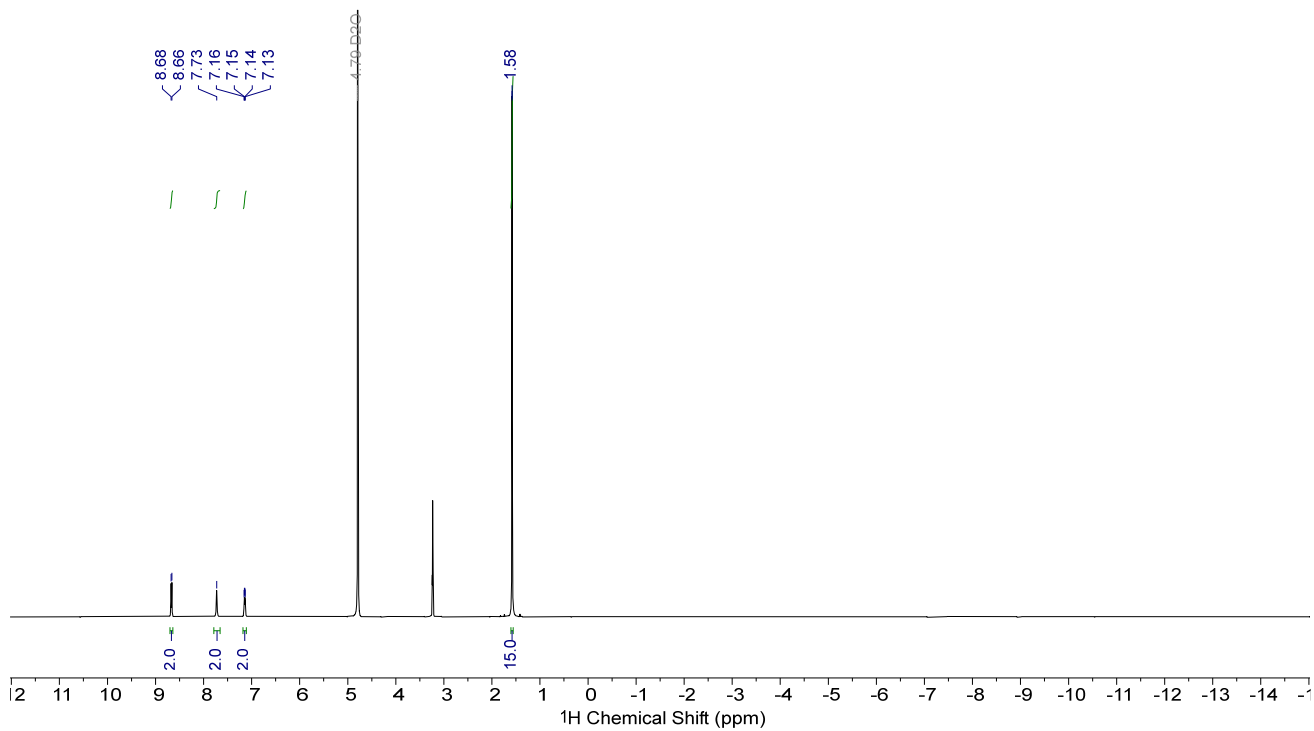


Figure S25. ^1H NMR of Ir1.

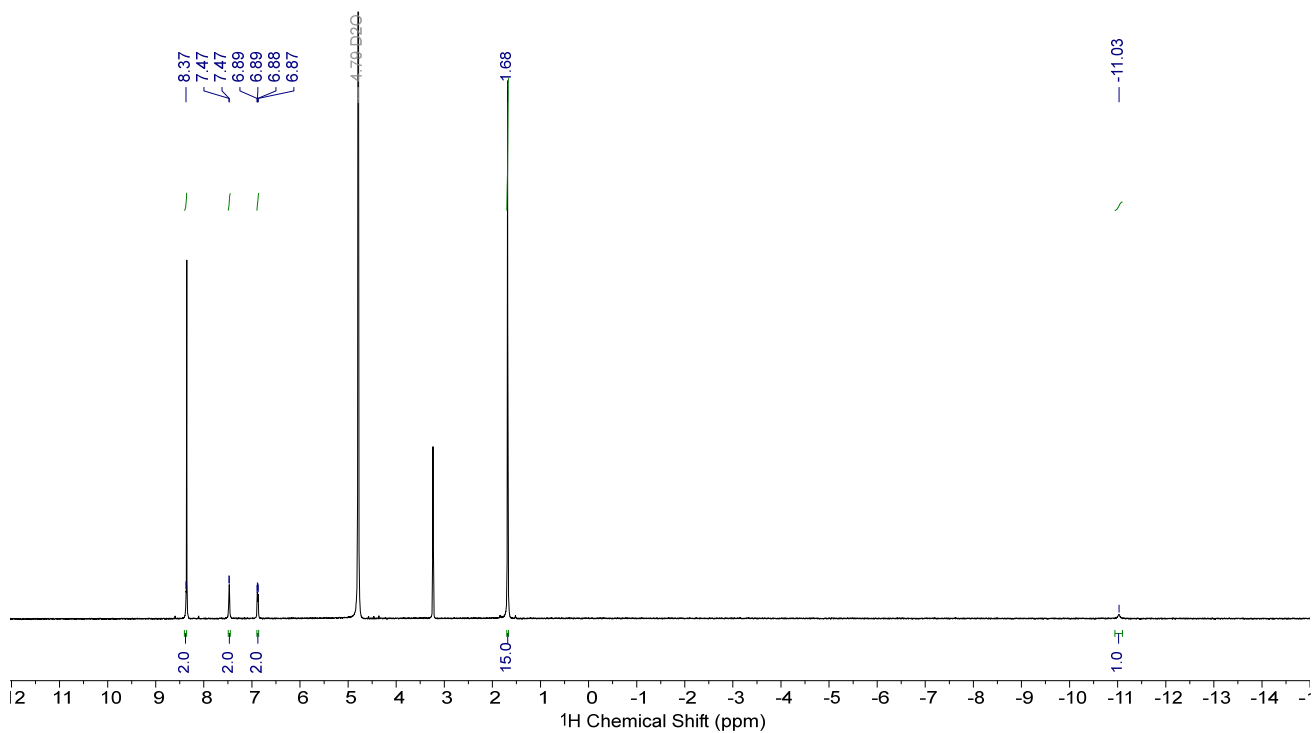


Figure S26. ^1H NMR of Ir1 with the addition of HCO_2K .

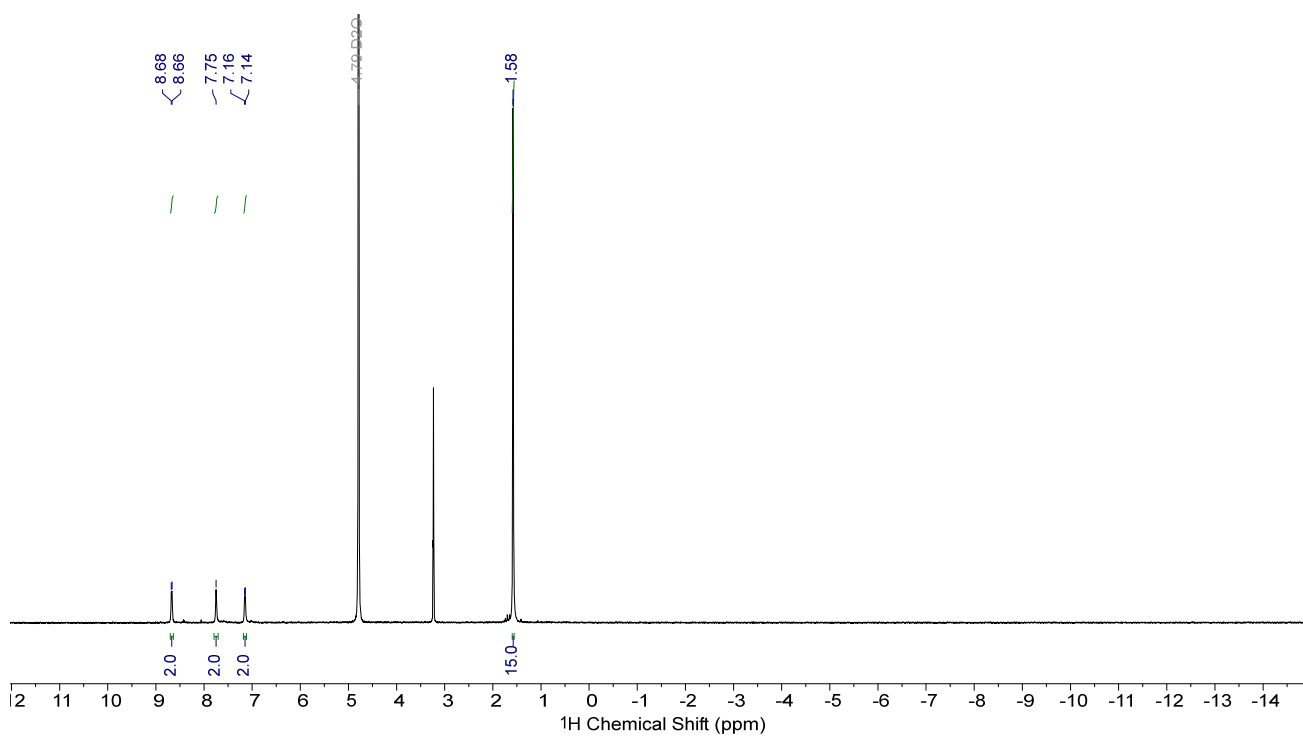


Figure S27. ¹H NMR of Ir1 with the addition of HCO₂K and D₂SO₄.

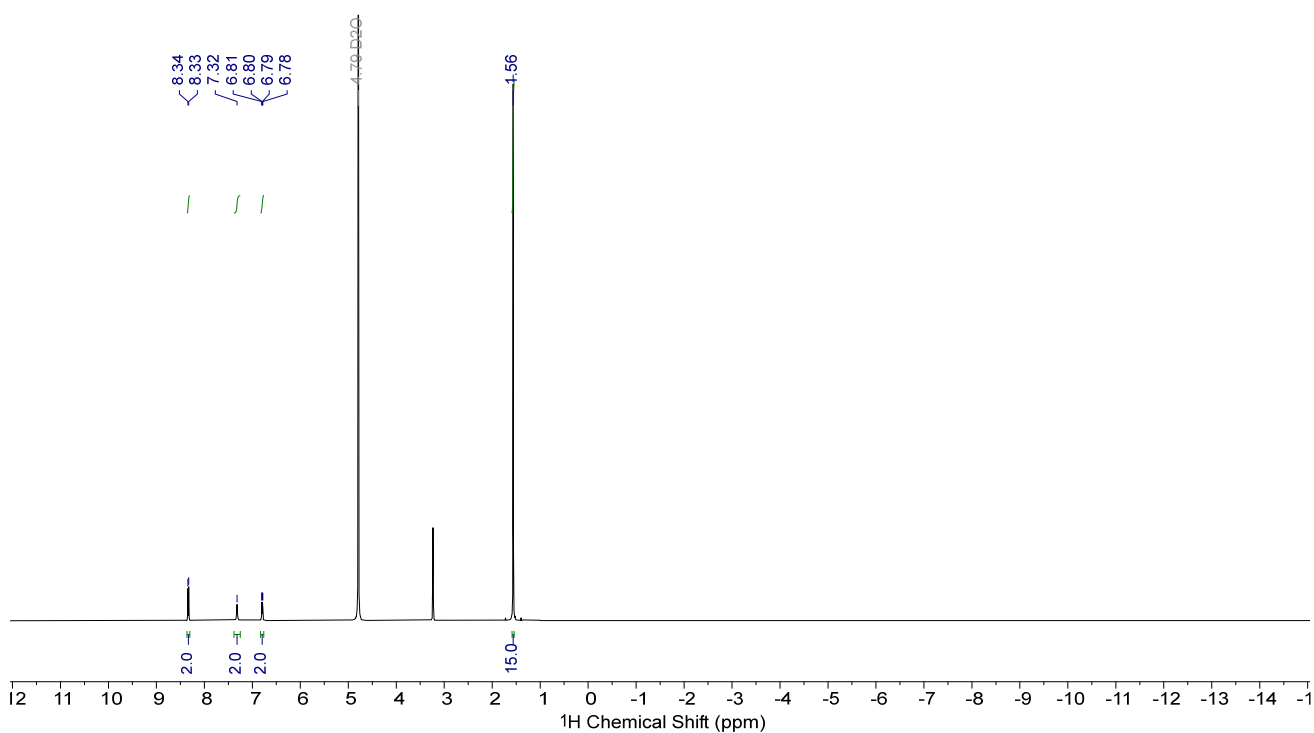


Figure S28. ¹H NMR of Ir2.

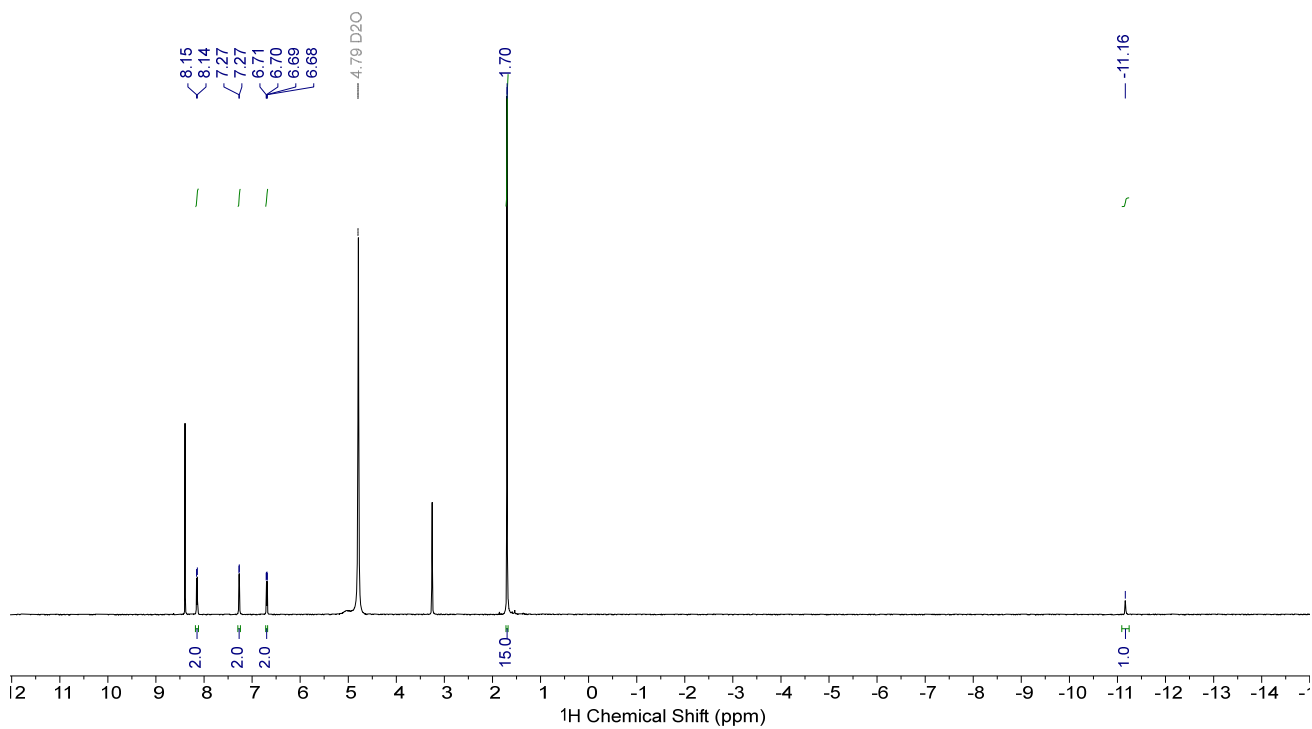


Figure S29. ^1H NMR of **Ir2** with the addition of HCO_2K .

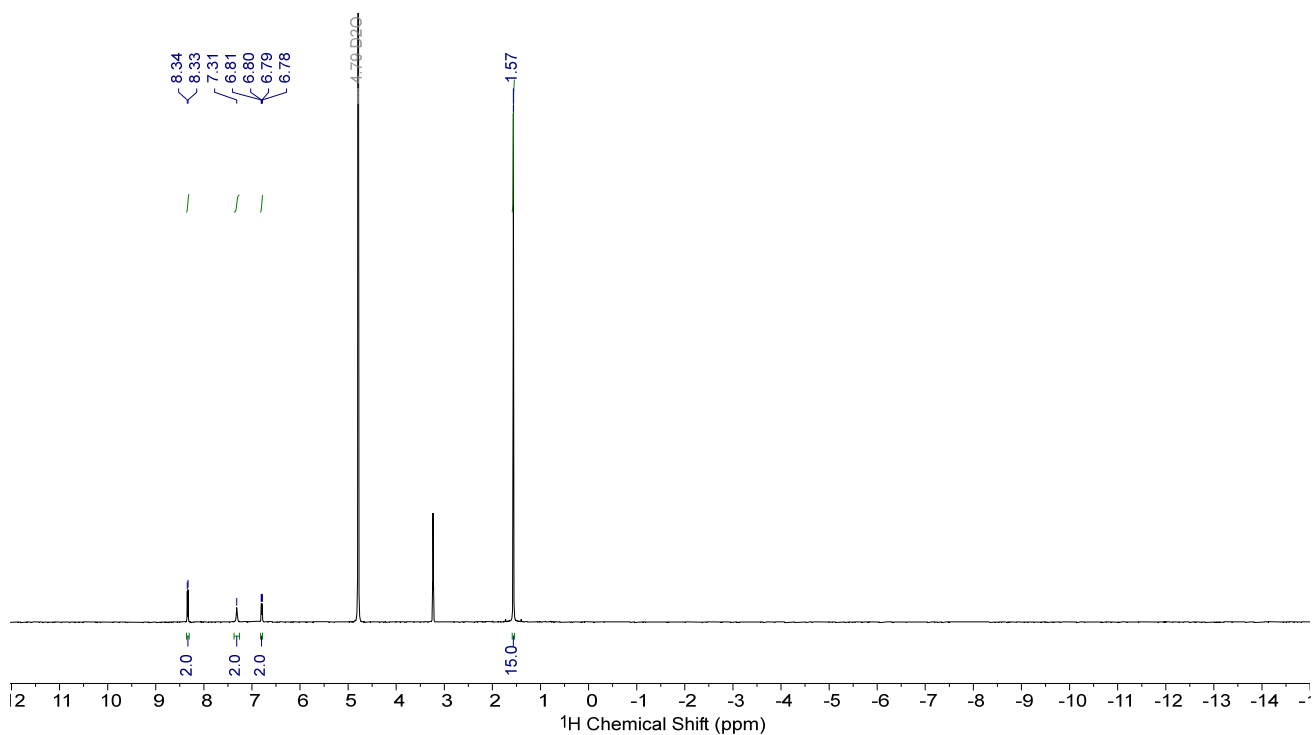


Figure S30. ^1H NMR of **Ir2** with the addition of HCO_2K and D_2SO_4 .

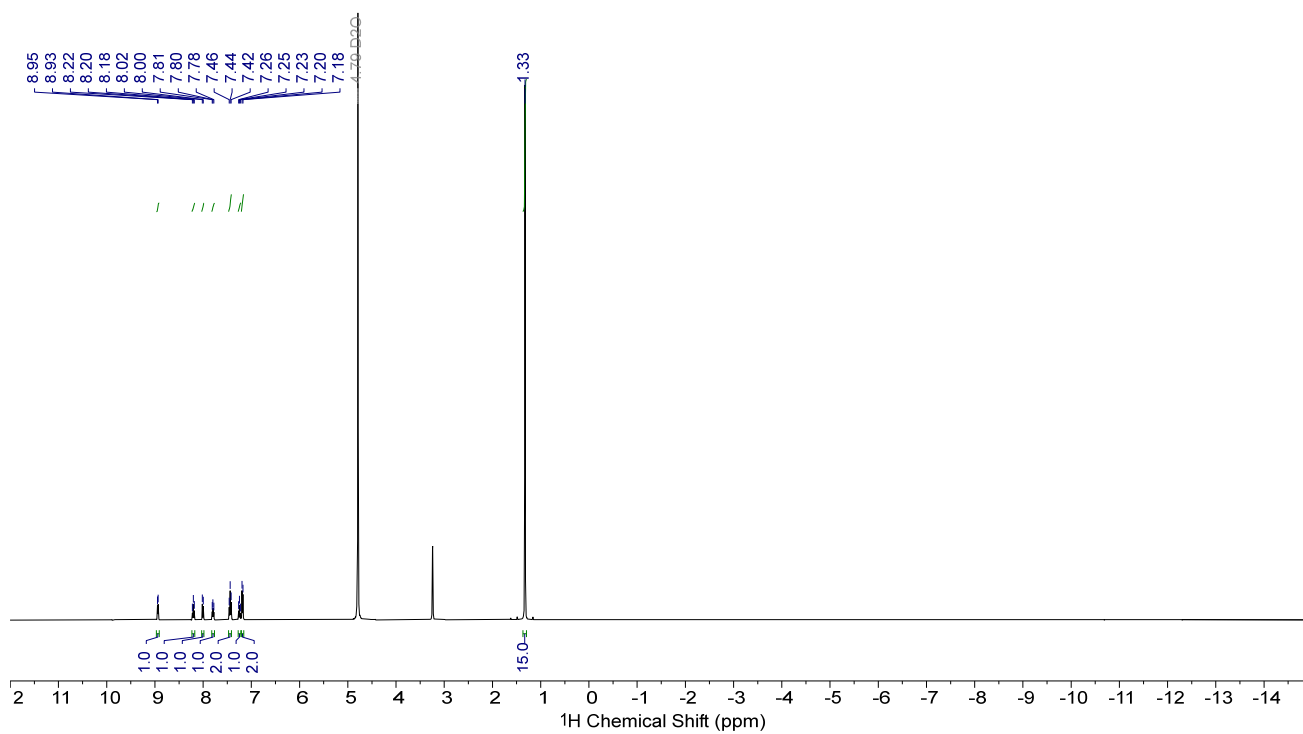


Figure S31. ^1H NMR of Ir3.

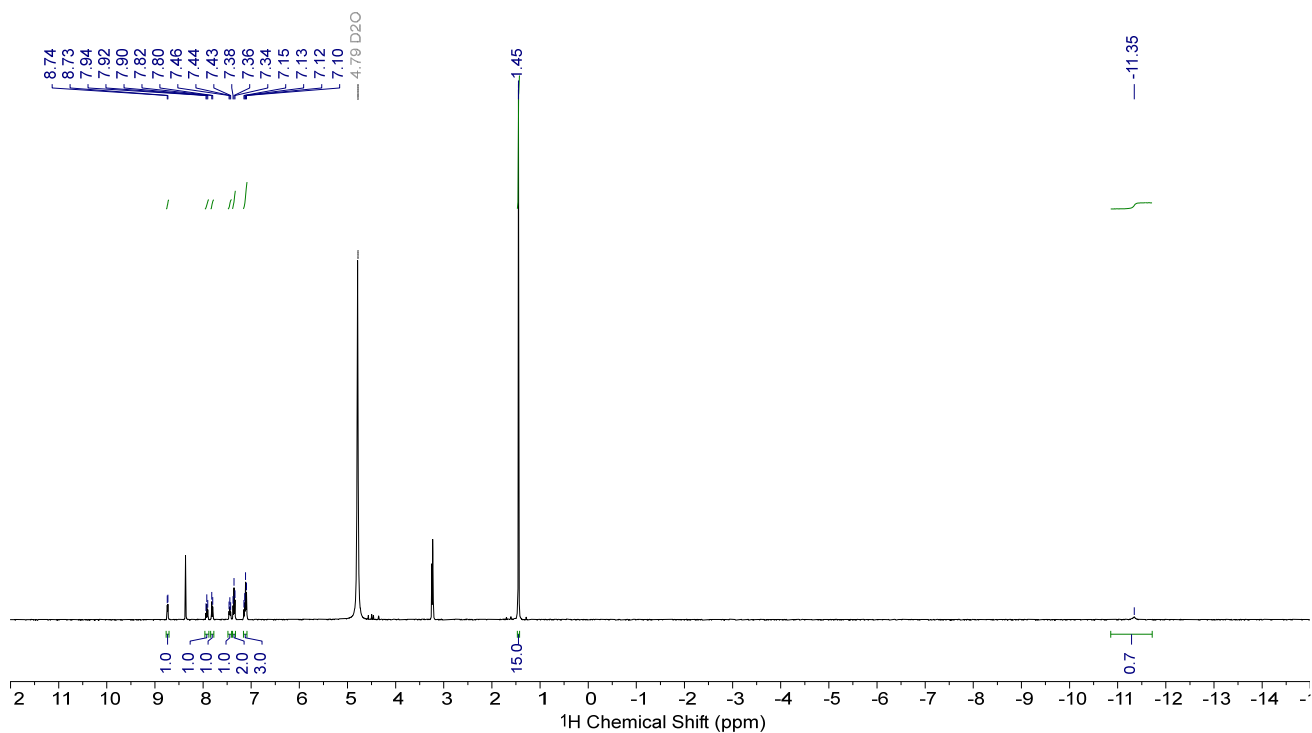


Figure S32. ^1H NMR of Ir3 with the addition of HCO_2K .

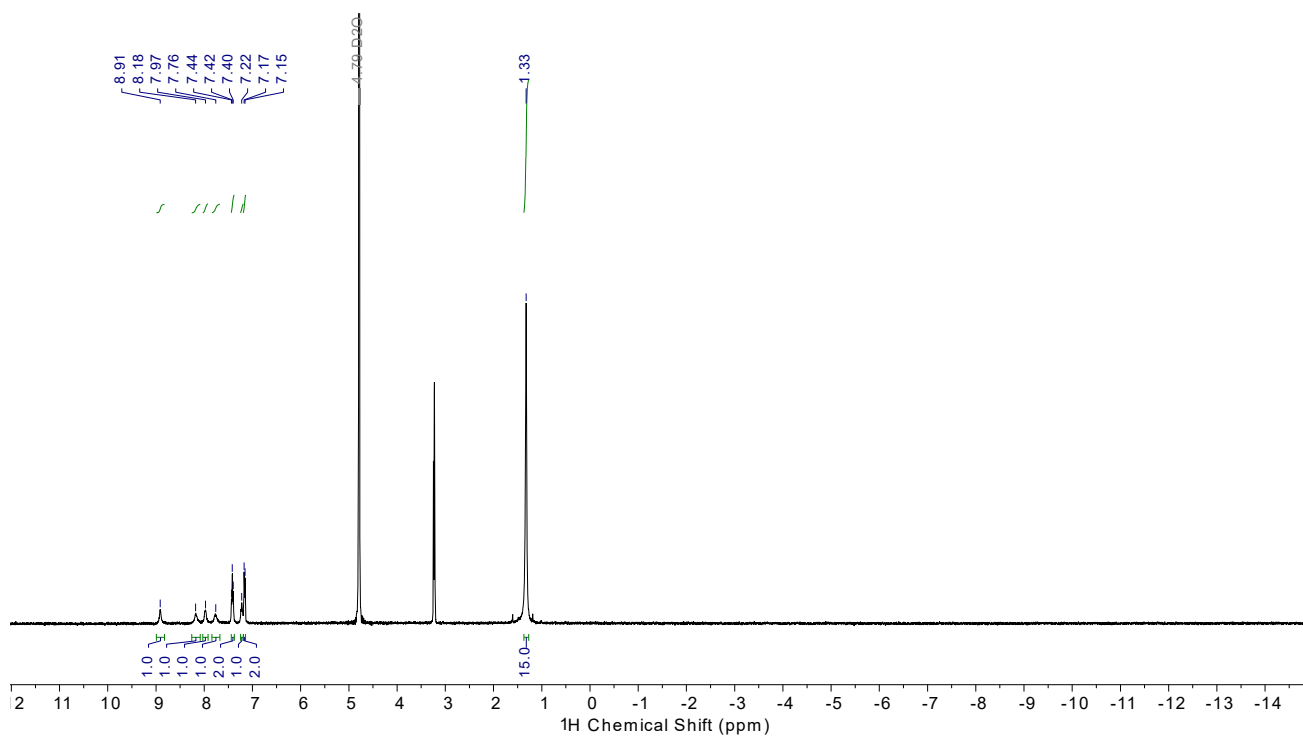


Figure S33. ^1H NMR of **Ir3** with the addition of HCO_2K and D_2SO_4 .

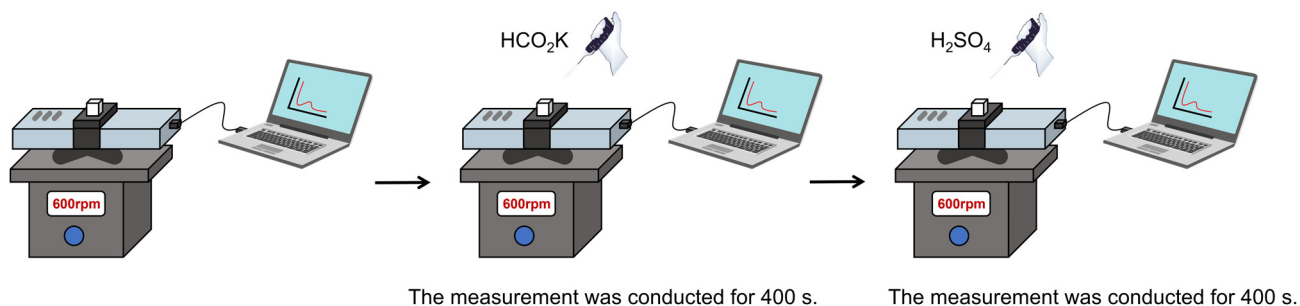


Figure S34. Schematic of in-situ UV-Vis spectroscopic analysis setup. UV-vis spectra were recorded at 25 °C on SEC2000 spectrometer with a charge coupled device array detector (ALS Co., Ltd). The solution was stirred at 600 rpm using a magnetic stirrer.